

## Triphenylphosphine-substituted selenido and sulfido clusters of osmium derived from $\text{Ph}_3\text{P}=\text{Se}$ or $\text{Ph}_3\text{P}=\text{S}$

Hamida Akter <sup>a</sup>, Antony J. Deeming <sup>\*,b</sup>, G.M. Golzar Hossain <sup>c</sup>, Shariff E. Kabir <sup>a,\*</sup>,  
Dwijendro N. Mondol <sup>a</sup>, Ebbe Nordlander <sup>d</sup>, Ayesha Sharmin <sup>a</sup>, Derek A. Tocher <sup>b</sup>

<sup>a</sup> Department of Chemistry, Jahangirnagar University, Savar, Dhaka 1342, Bangladesh

<sup>b</sup> Department of Chemistry, University College London, 20 Gordon Street, London WC1H 0AJ, UK

<sup>c</sup> Department of Chemistry, Cardiff University, P.O. Box 912, Cardiff CF10 3TB, UK

<sup>d</sup> Inorganic Chemistry, Center for Chemistry and Chemical Engineering, Lund University, Box 124, S-22100 Lund, Sweden

Received 24 June 2005; received in revised form 8 July 2005; accepted 11 July 2005

Available online 24 August 2005

### Abstract

Cleavage of  $\text{P}=\text{Se}$  bonds occurs readily in the room-temperature treatment of  $[\text{Os}_3(\text{CO})_{10}(\text{MeCN})_2]$  with  $\text{Ph}_3\text{P}=\text{Se}$  to give three new compounds,  $[\text{Os}_3(\mu_3\text{-Se})_2(\text{CO})_8(\text{PPh}_3)]$  (**2**),  $[\text{Os}_3(\mu_3\text{-Se})(\mu_3\text{-CO})(\text{CO})_7(\text{PPh}_3)_2]$  (**5**) and  $[\text{Os}_3(\mu\text{-OH})_2(\text{CO})_8(\text{PPh}_3)_2]$  (**6**), respectively, and three known compounds,  $[\text{Os}_3(\mu_3\text{-Se})_2(\text{CO})_9]$  (**1**),  $[\text{Os}_3(\mu_3\text{-Se})(\mu\text{-CO})_2(\text{CO})_7(\text{PPh}_3)]$  (**3**), and  $1,2\text{-}[\text{Os}_3(\text{CO})_{10}(\text{PPh}_3)_2]$  (**4**). No evidence for any product containing a co-ordinated  $\text{Ph}_3\text{P}=\text{Se}$  ligand was obtained. The analogous reaction between  $[\text{Os}_3(\text{CO})_{10}(\text{MeCN})_2]$  and  $\text{Ph}_3\text{P}=\text{S}$  produces five new compounds  $[\text{Os}_3(\mu_3\text{-S})_2(\text{CO})_8(\text{PPh}_3)]$  (**7**),  $[\text{Os}_3(\mu_3\text{-S})(\mu\text{-CO})_2(\text{CO})_7(\text{PPh}_3)]$  (**8**),  $[\text{Os}_3(\mu_3\text{-S})(\mu_3\text{-CO})(\text{CO})_7(\text{PPh}_3)_2]$  (**9**),  $[\text{Os}_3(\mu_3\text{-})_2(\text{CO})_7(\text{PPh}_3)_2]$  (**11**) and compound **6** in addition to the known compound **4**. Treatment of **2** with  $\text{Me}_3\text{NO}$  at  $50^\circ\text{C}$  gives the trinuclear cluster  $[\text{Os}_3(\mu_3\text{-Se})_2(\text{CO})_7(\text{PPh}_3)(\text{NMe}_3)]$  (**13**) and the hexanuclear cluster  $[\text{Os}_6(\mu_3\text{-Se})_4(\text{CO})_{14}(\text{PPh}_3)_2]$  (**12**). Treatment of compound **1** with  $\text{PPh}_3$  and  $\text{Me}_3\text{NO}$  at room temperature gives  $[\text{Os}_3(\mu_3\text{-Se})_2(\text{CO})_7(\text{PPh}_3)_2]$  (**10**). Compound **2** reacts with  $\text{PPh}_3$  similarly to give **10**. Compound **3** reacts with elemental selenium at  $110^\circ\text{C}$  to give **2**. The new compounds **2**, **5**, **6** and **8** were characterized by single-crystal X-ray diffraction. The compounds **3**, **5**, **8** and **9** contain  $\text{Os}_3(\mu_3\text{-S})$  or  $\text{Os}_3(\mu_3\text{-Se})$  cluster cores with three metal–metal bonds while **2**, **7**, **10**, **11** and **12** contain  $\text{Os}_3(\mu_3\text{-S})$  or  $\text{Os}_3(\mu_3\text{-Se})_2$  cores with two metal–metal bonds. The two hydroxy ligands in the triosmium cluster **6** bridging the open osmium–osmium edge and are probably derived from water. A study of the dynamic exchange of  $\text{PPh}_3$  ligands in **5** is also reported.

© 2005 Elsevier B.V. All rights reserved.

**Keywords:** Osmium carbonyl clusters; Triphenylphosphine selenide; Triphenylphosphine sulfide; Crystal structures

### 1. Introduction

Having a high affinity for later transition metals, chalcogen atoms are readily incorporated into transition-metal carbonyl clusters [1]. Many different coordination modes and geometries of the chalcogen atoms are

adopted and the triply-bridging sulfido ligand in particular has been exploited for the purpose of cluster growth [2,3]. The larger tellurium atom stabilizes triangular and square arrays of metal atoms [4]. Selenido ligands should be similarly useful but have been studied rather less [5]. Lewis et al. [6] reported that  $[\text{Os}_3(\text{CO})_{12}]$  reacts with elemental chalcogens in refluxing octane to give  $[\text{Os}_3(\mu\text{-H})_2(\mu_3\text{-X})(\text{CO})_9]$ ,  $[\text{Os}_3(\mu_3\text{-X})_2(\text{CO})_9]$  and  $[\text{Os}_4(\mu\text{-H})_2(\mu_3\text{-X})_2(\text{CO})_{12}]$  ( $\text{X} = \text{S}, \text{Se}$  or  $\text{Te}$ ), but a  $\text{CO}/\text{H}_2$  pressure is required to prepare the ruthenium analogues  $[\text{Ru}_3(\mu\text{-H})_2(\mu_3\text{-X})(\text{CO})_9]$  and  $[\text{Ru}_3(\mu_3\text{-X})_2(\text{CO})_9]$ . It has recently been reported that the treatment of Fe and Ru

\* Corresponding author. Present address: Department of Chemistry, University of Montana, 32 Campus Drive, Missoula, MT 59812, USA. Tel.: +1 406 243 2592; fax: +1 406 243 2477.

E-mail addresses: [a.j.deeming@ucl.ac.uk](mailto:a.j.deeming@ucl.ac.uk) (A.J. Deeming), [skabir\\_ju@yahoo.com](mailto:skabir_ju@yahoo.com) (S.E. Kabir).



Table 1  
Crystal data and structure refinement for **2**, **5**, **6** and **8**

Complex	<b>2</b>	<b>5</b>	<b>6</b>	<b>8</b>
Chemical formula	C <sub>26</sub> H <sub>15</sub> O <sub>8</sub> Os <sub>3</sub> PSe <sub>2</sub>	C <sub>44</sub> H <sub>30</sub> O <sub>8</sub> Os <sub>3</sub> P <sub>2</sub> Se · CH <sub>2</sub> Cl <sub>2</sub>	C <sub>44</sub> H <sub>32</sub> O <sub>10</sub> Os <sub>3</sub> P <sub>2</sub>	C <sub>27</sub> H <sub>15</sub> O <sub>9</sub> Os <sub>3</sub> PS
Formula weight	1214.87	1483.11	1353.24	1117.02
<i>T</i> (K)	293(2)	150(2)	150(2)	150(2)
$\lambda$ (Å)	0.71073	0.71073	0.71073	0.71073
Space group	<i>P</i> $\bar{1}$	<i>P</i> $\bar{1}$	<i>P</i> 2 <sub>1</sub> / <i>n</i>	<i>P</i> 2 <sub>1</sub> / <i>n</i>
Unit cell parameters				
<i>a</i> (Å)	8.8222(6)	10.60210(10)	13.1197(6)	14.7118(9)
<i>b</i> (Å)	12.6657(9)	11.3496(2)	17.8055(8)	9.6925(6)
<i>c</i> (Å)	14.7417(10)	20.3179(3)	17.5309(18)	20.3593(12)
$\alpha$ (°)	69.4710(10)	89.7097(8)	90	90
$\beta$ (°)	76.5650(10)	87.1785(8)	94.4190(10)	99.2290(10)
$\gamma$ (°)	83.0960(10)	66.6625(6)	90	90
<i>V</i> (Å <sup>3</sup> )	1499.05(18)	2241.83(6)	4081.4(3)	2865.5(3)
<i>Z</i>	2	2	4	4
<i>D</i> <sub>calc</sub> (g/cm <sup>3</sup> )	2.691	2.197	2.202	2.589
Absorption coefficient $\mu$ (mm <sup>-1</sup> )	15.209	9.359	9.455	13.450
<i>F</i> (000)	1092	1384	2536	2032
Crystal size (mm <sup>3</sup> )	0.44 × 0.21 × 0.14	0.24 × 0.16 × 0.16	0.23 × 0.15 × 0.08	0.38 × 0.16 × 0.12
$\theta$ Range for data collection (°)	1.72–28.29	2.95–27.49	1.87–28.29	1.59–28.30
Index ranges	–11 ≤ <i>h</i> ≤ 11, –16 ≤ <i>k</i> ≤ 16, –18 ≤ <i>l</i> ≤ 19	–13 ≤ <i>h</i> ≤ 13, –23 ≤ <i>k</i> ≤ 23, –26 ≤ <i>l</i> ≤ 26	–17 ≤ <i>h</i> ≤ 17, –14 ≤ <i>k</i> ≤ 14, –22 ≤ <i>l</i> ≤ 22	–18 ≤ <i>h</i> ≤ 18, –12 ≤ <i>k</i> ≤ 12, <i>l</i> –27 ≤ <i>l</i> ≤ 27
Reflection collected	13307	37690	35789	24769
Independent reflections	6906	10185	9715	6834
<i>R</i> <sub>int</sub>	0.0388	0.0772	0.0283	0.0361
Reflections with <i>F</i> <sup>2</sup> > 2 $\sigma$	5942	8989	8989	6419
Minimum and maximum transmission	0.0573 and 0.2333	0.3107 and 0.2081	0.2197 and 0.5184	0.0799 and 0.2952
Refinement method	Full-matrix least-square on <i>F</i> <sup>2</sup>	Full-matrix least-square on <i>F</i> <sup>2</sup>	Full-matrix least-square on <i>F</i> <sup>2</sup>	Full-matrix least-square on <i>F</i> <sup>2</sup>
Data/restraints/parameters	6906/0/463	10185/0/550	9715/0/540	6834/0/371
<i>R</i> indices [ <i>F</i> <sup>2</sup> > 2 $\sigma$ ]	<i>R</i> <sub>1</sub> = 0.0465, <i>wR</i> <sub>2</sub> = 0.1125	<i>R</i> <sub>1</sub> = 0.0387, <i>wR</i> <sub>2</sub> = 0.0919	<i>R</i> <sub>1</sub> = 0.0221, <i>wR</i> <sub>2</sub> = 0.0430	<i>R</i> <sub>1</sub> = 0.0274, <i>wR</i> <sub>2</sub> = 0.0560
<i>R</i> indices (all data)	<i>R</i> <sub>1</sub> = 0.0540, <i>wR</i> <sub>2</sub> = 0.1178	<i>R</i> <sub>1</sub> = 0.0498, <i>wR</i> <sub>2</sub> = 0.0978	<i>R</i> <sub>1</sub> = 0.0255, <i>wR</i> <sub>2</sub> = 0.0439	<i>R</i> <sub>1</sub> = 0.0304, <i>wR</i> <sub>2</sub> = 0.0572
Goodness-of-fit on <i>F</i> <sup>2</sup>	1.042	1.012	1.087	1.172
Largest and mean shift (su)	0.000 and 0.000	0.000 and 0.000	0.004 and 0.000	0.001 and 0.000
Largest difference in peak and hole (e Å <sup>-3</sup> )	2.189 and –3.071	2.776 and –2.489	0.876 and –0.767	2.515 and –0.945

any clusters with co-ordinated  $\text{Ph}_3\text{P}=\text{Se}$  ligands so the  $\text{P}=\text{Se}$  bond cleavage to give selenido clusters must occur rapidly following coordination. This observation is different from that of Ho and Wong [12] who reported  $[\text{Os}_3(\text{CO})_{10}\{\text{Ph}_2(\text{SH})\text{NP}(\text{S})\text{Ph}_2\text{-S,S}\}]$  and  $[(\mu\text{-H})\text{Os}_3(\text{CO})_9\{\text{Ph}_2\text{P}(\text{S})\text{NP}(\text{S})\text{Ph}_2\text{-S,S}\}]$  containing undissociated bis(diphenylthiophosphinoyl)amine ligand from the reaction between  $[\text{Os}_3(\text{CO})_{10}(\text{MeCN})_2]$  and  $\text{Ph}_2\text{P}(\text{S})\text{-NHP}(\text{S})\text{Ph}_2$ . The new compounds **2**, **5** and **6** have been characterized spectroscopically and by single-crystal X-ray diffraction. The solid-state molecular structure of **2** (Fig. 1 and Table 2) consists of an open  $\text{Os}_3$  cluster with two metal–metal bonds, eight terminal CO, a  $\text{PPh}_3$  and two triply-bridging selenido ligands. The structure was refined with two equally populated disordered orientations of the phenyl groups as shown superimposed in Fig. 1. Both disordered arrangements have the same  $\text{Os}_3(\mu_3\text{-Se})_2(\text{CO})_8\text{P}$  core structure and small variations within the core as a result of the disorder are believed to be insignificant.

The two  $\text{Os}\text{-Os}$  distances in **2** [ $\text{Os}(1)\text{-Os}(3) = 2.7741(5)$  and  $\text{Os}(2)\text{-Os}(3) = 2.8551(5)$  Å] are rather different, with that involving  $\text{Os}(2)$  bound to the  $\text{PPh}_3$  ligand being longer. The  $\text{Os}(1)\cdots\text{Os}(2)$  separation at 3.833 Å is similar to that observed in  $[\text{Os}_3(\mu_3\text{-Se})_2(\text{CO})_6(\mu\text{-dppm})(\text{PPh}_3)]$  [3.835 Å] [10] but is significantly longer than that in  $[\text{Os}_3(\mu_3\text{-S})_2(\text{CO})_9]$  [3.662(1) Å] [13].

The  $\text{Os}_3\text{Se}_2$  core is square pyramidal with two Os and two Se atoms alternating in base and the third Os atom at the vertex. The two Se atoms cap the Os triangle asymmetrically. The  $\text{Os}\text{-Se}$  distances to the central seven-coordinate metal atom  $\text{Os}(3)$  [ $\text{Os}(3)\text{-Se}(1) =$

Table 2

Selected bond distances (Å) and angles (°) for  $[\text{Os}_3(\mu_3\text{-Se})_2(\text{CO})_8(\text{PPh}_3)]$  (**2**)

$\text{Os}(1)\text{-Os}(3)$	2.7741(5)
$\text{Os}(2)\text{-Os}(3)$	2.8551(5)
$\text{Os}(1)\text{-Se}(1)$	2.5074(10)
$\text{Os}(2)\text{-Se}(2)$	2.4893(11)
$\text{Os}(2)\text{-Se}(1)$	2.5066(9)
$\text{Os}(3)\text{-Se}(1)$	2.5535(9)
$\text{Os}(3)\text{-Se}(2)$	2.5525(10)
$\text{Os}(1)\text{-Se}(2)$	2.5064(11)
$\text{Os}(2)\text{-P}(1)$	2.310(2)
$\text{P}(1)\text{-Os}(2)\text{-Se}(2)$	104.21(6)
$\text{P}(1)\text{-Os}(2)\text{-Se}(1)$	106.15(5)
$\text{Os}(1)\text{-Os}(3)\text{-Os}(2)$	85.810(13)
$\text{Se}(1)\text{-Os}(1)\text{-Os}(3)$	57.56(2)
$\text{Se}(2)\text{-Os}(2)\text{-Se}(1)$	80.10(3)
$\text{Se}(1)\text{-Os}(3)\text{-Os}(1)$	55.97(2)
$\text{Se}(2)\text{-Os}(2)\text{-Os}(3)$	56.56(2)
$\text{Se}(2)\text{-Os}(3)\text{-Os}(2)$	54.47(2)
$\text{Os}(2)\text{-Se}(1)\text{-Os}(1)$	99.71(3)
$\text{Os}(2)\text{-Se}(1)\text{-Os}(3)$	68.69(2)
$\text{Os}(2)\text{-Se}(2)\text{-Os}(1)$	100.21(3)
$\text{Os}(1)\text{-Se}(2)\text{-Os}(3)$	66.50(3)
$\text{Se}(2)\text{-Os}(1)\text{-Se}(1)$	79.76(3)
$\text{Se}(2)\text{-Os}(1)\text{-Os}(3)$	57.54(3)
$\text{P}(1)\text{-Os}(2)\text{-Os}(3)$	153.82(5)
$\text{Se}(2)\text{-Os}(3)\text{-Se}(1)$	78.04(3)
$\text{Se}(2)\text{-Os}(3)\text{-Os}(1)$	55.95(3)
$\text{Se}(1)\text{-Os}(3)\text{-Os}(2)$	54.88(2)
$\text{Os}(1)\text{-Se}(1)\text{-Os}(3)$	66.47(2)
$\text{Os}(2)\text{-Se}(2)\text{-Os}(3)$	68.97(3)
$\text{Se}(1)\text{-Os}(2)\text{-Os}(3)$	56.43(2)

$2.5535(9)$  Å and  $\text{Os}(3)\text{-Se}(2) = 2.5525(10)$  Å] are longer than those to  $\text{Os}(1)$  and  $\text{Os}(2)$ , which are in the range 2.4893(11)–2.5074(10) Å. The  $\text{PPh}_3$  ligand is coordinated

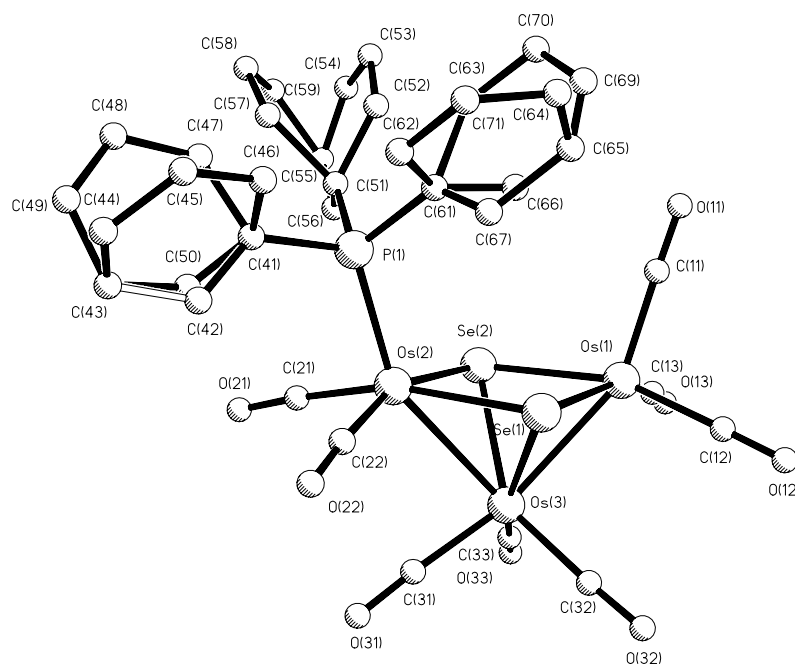


Fig. 1. Solid-state molecular structure of  $[\text{Os}_3(\mu_3\text{-Se})_2(\text{CO})_8(\text{PPh}_3)]$  (**2**) showing the two equally populated disordered arrangements of the phenyl groups of the  $\text{PPh}_3$  ligand.

at Os(2), *trans* to an Os–Os bond. The Os–P bond distance of 2.310(2) Å is comparable to that in  $[\text{Os}_3(\mu_3\text{-S})_2(\text{CO})_8(\text{PMe}_2\text{Ph})]$  [2.298(3) Å] [12], and overall, the structure is similar to that of this sulfur analogue. Spectroscopic data for **2** indicate that it retains its solid-state structure in solution. As expected the  $^{31}\text{P}\{^1\text{H}\}$  NMR spectrum of **2** is a singlet ( $\delta$  19.1) and the FAB mass spectrum contains the molecular ion peak at  $m/z$  1216.

The solid-state molecular structure of  $[\text{Os}_3(\mu_3\text{-Se})(\mu_3\text{-CO})(\text{CO})_7(\text{PPh}_3)_2]$  (**5**) (Fig. 2 and Table 3) consists of three mutually bonded Os atoms with a triply-bridging CO, seven terminal CO, a triply-bridging Se and two  $\text{PPh}_3$  ligands. The Os–Os separations are only slightly different [ $\text{Os}(1)\text{--Os}(2) = 2.8418(3)$ ,  $\text{Os}(2)\text{--Os}(3) = 2.8752(3)$  and  $\text{Os}(1)\text{--Os}(3) = 2.8917(3)$  Å]. Each Os atom has a different co-ordination sphere and the phosphine ligands are co-ordinated inequivalently; P(1) is *trans* to Se(1) while P(2) is *cis* to Se(1). The tetrahedral  $\text{Os}_3\text{Se}$  core contains a symmetrically capped Se atom [ $\text{Os}(1)\text{--Se}(1) = 2.5140(6)$  Å,  $\text{Os}(2)\text{--Se}(1) = 2.5093(6)$  Å,  $\text{Os}(3)\text{--Se}(1) = 2.5101(6)$  Å]. In contrast, the  $\mu_3\text{-CO}$  forms shorter bonds to the more electron-rich Os centers [ $\text{Os}(1)\text{--C}(8) = 2.193(6)$ ,  $\text{Os}(2)\text{--C}(8) = 2.154(6)$ ,  $\text{Os}(3)\text{--C}(8) = 2.141(6)$  Å].

The  $^{31}\text{P}\{^1\text{H}\}$  NMR spectrum of **5** ( $\text{CDCl}_3$  solution) at 223 K shows two equal intensity sharp singlets at  $\delta$  14.6 and  $-7.4$ , as expected for the molecular structure found in the crystal. However, at 323 K these signals have coalesced to a single resonance at  $\delta$  5.8 as a result of the interconversion of the two enantiomers **5a** and **5b** (Scheme 2). The calculated weighted-average signal would be at  $\delta$  3.6. Fig. 3 shows spectra over this temperature range with our best simulations using the program gNMR (Version 4.1, Cherwell Scientific, 1999) based on

Table 3

Selected bond distances (Å) and angles ( $^\circ$ ) for  $[\text{Os}_3(\mu_3\text{-Se})(\mu_3\text{-CO})(\text{CO})_7(\text{PPh}_3)_2] \cdot \text{CH}_2\text{Cl}_2$  (**5**)

Os(1)–Os(3)	2.8917(3)
Os(2)–Os(3)	2.8752(3)
Os(1)–Os(2)	2.8418(3)
Os(1)–Se(1)	2.5140(6)
Os(2)–Se(1)	2.5093(6)
Os(3)–Se(1)	2.5101(6)
Os(1)–C(8)	2.193(6)
Os(2)–C(8)	2.154(6)
Os(3)–C(8)	2.141(6)
Os(2)–P(1)	2.3528(15)
Os(2)–P(2)	2.3557(15)
Os(2)–Os(1)–Os(3)	60.188(8)
Os(1)–Os(2)–Os(3)	60.765(8)
Os(2)–Os(3)–Os(1)	68.905(16)
Se(1)–Os(3)–Os(2)	55.041(14)
Se(1)–Os(2)–Os(1)	55.625(15)
Se(1)–Os(2)–Os(3)	55.064(15)
Se(1)–Os(1)–Os(3)	54.797(15)
Se(1)–Os(1)–Os(2)	55.470(15)
Se(1)–Os(3)–Os(1)	54.925(15)
P(2)–Os(3)–Os(1)	99.32(4)
P(1)–Os(2)–Os(3)	122.67(4)
P(1)–Os(2)–Os(1)	111.89(4)
C(8)–Os(1)–Os(3)	47.40(15)
C(8)–Os(2)–Os(3)	47.80(15)
C(8)–Os(3)–P(2)	133.32(16)
C(8)–Os(3)–Se(1)	89.19(17)
C(8)–Os(3)–Os(2)	48.16(16)
C(8)–Os(1)–Se(1)	87.96(16)
C(8)–Os(1)–Os(2)	48.58(16)
P(2)–Os(3)–Se(1)	97.53(4)
C(8)–Os(2)–Se(1)	88.94(16)
P(2)–Os(3)–Os(2)	151.11(4)
C(8)–Os(3)–Os(1)	48.91(17)
Os(2)–Se(1)–Os(1)	68.905(16)
Os(2)–Se(1)–Os(3)	69.895(17)
Os(3)–Se(1)–Os(1)	70.278(17)

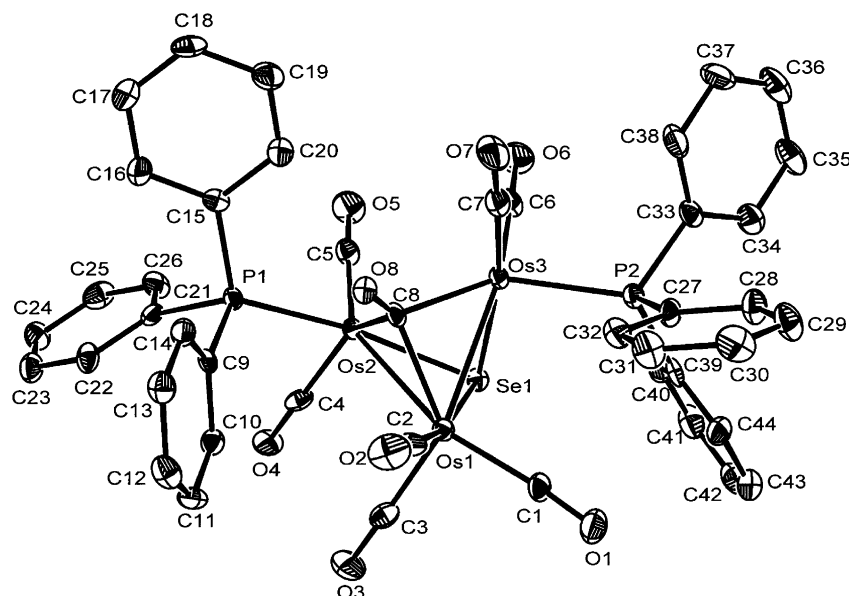
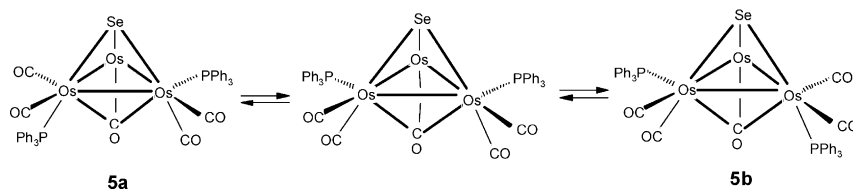


Fig. 2. Solid-state molecular structure of  $[\text{Os}_3(\mu_3\text{-Se})(\mu_3\text{-CO})(\text{CO})_7(\text{PPh}_3)_2]$  (**5**). Thermal ellipsoids are drawn at the 50% probability level.



Scheme 2.

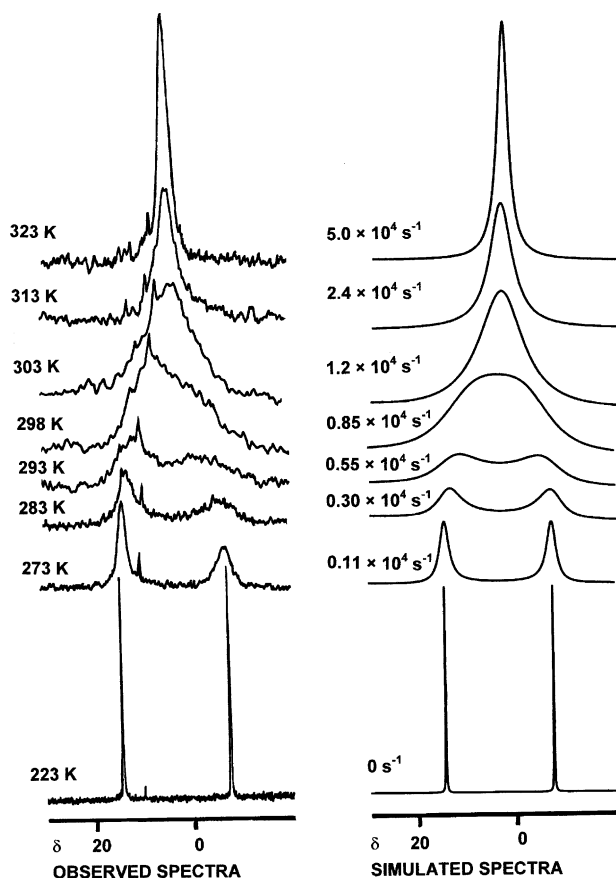


Fig. 3. Observed  $^{31}\text{P}\{^1\text{H}\}$  NMR spectra (162 MHz) of cluster **5** in  $\text{CDCl}_3$  solution and those simulated using the program *gNMR*. Spectra are annotated with temperatures and calculated rate coefficients.

site exchange between the two  $^{31}\text{P}$  nuclei. Activation parameters were determined [ $\Delta G^\ddagger = 50.4 \pm 0.8 \text{ kJ mol}^{-1}$  at 298 K;  $\Delta H^\ddagger = 51.4 \pm 0.9 \text{ kJ mol}^{-1}$ ;  $\Delta S^\ddagger = 3.2 \pm 6.2 \text{ J K}^{-1} \text{ mol}^{-1}$ ] but these data should be considered with caution because of the unsymmetrical nature of the coalescing signals was not modelled. Although only one isomer is detected at 223 K, we believe that at higher temperatures there is a partial population of another isomer or isomers in equilibrium with the main isomer found in the crystal leading to distortion.

Scheme 2 is a possible mechanism. A symmetrical intermediate in the conversion of the enantiomers **5a** to **5b** such as that shown may be partially populated leading to the distortion of the coalescing signals. If this is correct, turnstile rotations of the two  $\text{Os}(\text{CO})_2(\text{PPh}_3)$

groups would then not occur synchronously but as separate processes.

The molecular structure of **6** (Fig. 4 and Table 4) consists of an open triangular cluster of three Os atoms with eight terminal CO, two bridging OH and two  $\text{PPh}_3$  ligands. The non-bonded  $\text{Os}(1)\cdots\text{Os}(2)$  distance of  $3.1197(2) \text{ \AA}$  is significantly longer than the  $\text{Os}(1)\text{--Os}(3)$  and  $\text{Os}(2)\text{--Os}(3)$  distances [ $2.8572(2)$  and  $2.8585(2) \text{ \AA}$ ]. The three metal atoms are electron-precise without the  $\text{Os}(1)\text{--Os}(2)$  bond. Both OH groups symmetrically span the open  $\text{Os}(1)\cdots\text{Os}(2)$  edge and the Os–O distances [ $\text{Os}(1)\text{--O}(1) = 2.140(2)$ ,  $\text{Os}(1)\text{--O}(2) = 2.148(2)$ ,  $\text{Os}(2)\text{--O}(1) = 2.126(2)$  and  $\text{Os}(2)\text{--O}(2) = 2.141(2) \text{ \AA}$ ] are comparable to the Os–O distances in other OH-bridged triosmium clusters: [ $\text{Os}_3(\mu\text{-H})(\mu\text{-OH})(\text{CO})_{10}$ ] [ $2.146(7)$ ,  $2.136(7) \text{ \AA}$ ] [14] [ $\text{Os}_3(\mu\text{-H})(\mu\text{-OH})(\text{CO})_9(\text{PMe}_2\text{Ph})$ ] [ $2.135(5)$ ,  $2.118(5) \text{ \AA}$ ] [15] and [ $\text{Os}_3(\mu\text{-H})(\mu\text{-OH})(\text{CO})_8(\mu\text{-dppm})$ ] [ $2.157(8)$ ,  $2.167(8) \text{ \AA}$ ] [16]. We believe that the shortness of the non-bonded  $\text{Os}(1)\cdots\text{Os}(2)$  edge is attributed to the presence of two light-atom bridges. A similar shortening of the open edges has been reported in [ $\text{Ru}_3(\mu\text{-OH})_2(\text{CO})_8(\mu\text{-BINAP})$ ] [ $3.023(2) \text{ \AA}$ ] [17] and [ $\text{Ru}_3(\mu\text{-OH})_2(\text{CO})_8\{\mu\text{-}\eta^2\text{-Fe}(\text{C}_5\text{H}_4\text{PPh}_2)_2\}$ ] [ $3.0358(8) \text{ \AA}$ ] [18]. The good quality X-ray data allowed us to locate the hydroxy H-atoms. One is *exo* and the other *endo* with respect to the  $\text{Os}(\text{CO})_4$  group. Although this makes the OH bridges inequivalent there is no evidence for this in positions of the oxygen atoms. The origin of the hydroxy ligands in **6** may be dioxygen or more likely water and there are examples of the formation of OH ligands in triosmium and triruthenium clusters from water or dioxygen [19–21].

In spite of their inequivalence in the solid-state structure, the OH protons in **6** give a single triplet at  $\delta -0.18$  ( $J_{\text{PH}} = 3.6 \text{ Hz}$ ) in the  $^1\text{H}$  NMR spectrum. The high-field chemical shift and  $J_{\text{PH}}$  for the OH protons in **6** are in the range of values found for other structurally characterized OH-bridged trimetallic clusters: [ $\text{Ru}_3(\mu\text{-OH})_2(\text{CO})_8(\mu\text{-BINAP})$ ] [ $\delta -1.48$ ,  $J_{\text{PH}} = 4.0 \text{ Hz}$ ] [17], [ $\text{Ru}_3(\mu\text{-OH})_2(\text{CO})_8\{\mu\text{-}\eta^2\text{-Fe}(\text{C}_5\text{H}_4\text{PPh}_2)_2\}$ ] [ $\delta -0.68$ ,  $J_{\text{PH}} = 4.0 \text{ Hz}$ ] [18], [ $\text{Os}_3(\mu\text{-H})(\mu\text{-OH})(\text{CO})_8(\mu\text{-dppm})$ ] [ $\delta 0.44$ ,  $J_{\text{PH}} = 4.3 \text{ Hz}$ ] [16] and [ $\text{Os}_3(\mu\text{-OH})(\mu\text{-MeOCO})(\text{CO})_9(\text{PPh}_3)$ ] [ $\delta -1.98$ ,  $J_{\text{PH}} = 4.8 \text{ Hz}$ ] [22]. The  $^{31}\text{P}\{^1\text{H}\}$  NMR singlet at  $\delta 11.6$  indicates that the  $^{31}\text{P}$  nuclei are equivalent. The FAB MS shows the parent ion at  $m/z$  1354 and IR spectrum contains a broad absorption at  $3505 \text{ cm}^{-1}$ , assignable to  $\nu(\text{OH})$ .

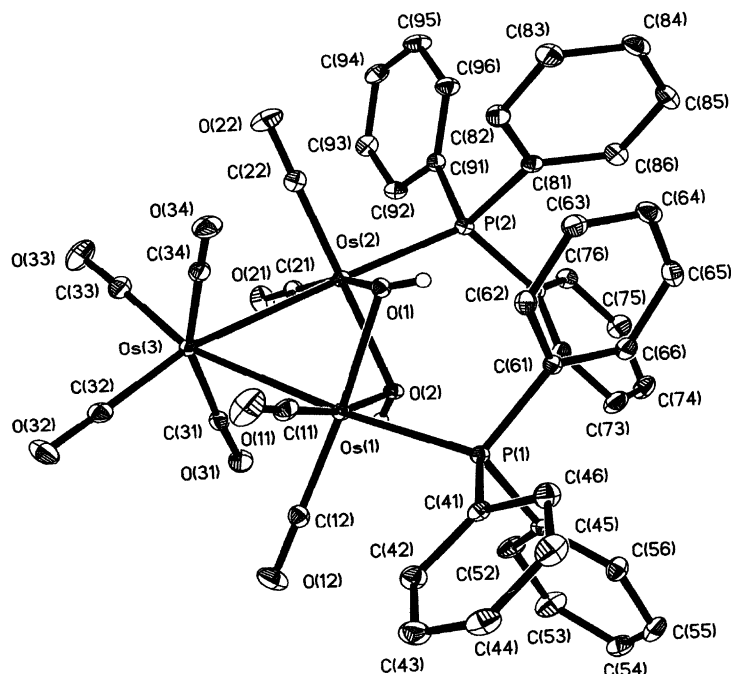


Fig. 4. Solid-state molecular structure of  $[\text{Os}_3(\mu\text{-OH})_2(\text{CO})_8(\text{PPh}_3)_2]$  (**6**). Thermal ellipsoids are drawn at the 50% probability level.

The corresponding treatment of  $[\text{Os}_3(\text{CO})_{10}(\text{MeCN})_2]$  with  $\text{Ph}_3\text{P}=\text{S}$  at room temperature gives five new compounds  $[\text{Os}_3(\mu_3\text{-S})_2(\text{CO})_8(\text{PPh}_3)]$  (**7**),  $[\text{Os}_3(\mu_3\text{-Se})(\mu\text{-CO})_2(\text{CO})_7(\text{PPh}_3)]$  (**8**),  $[\text{Os}_3(\mu_3\text{-S})(\mu\text{-CO})(\text{CO})_7(\text{PPh}_3)_2]$  (**9**),  $[\text{Os}_3(\mu_3\text{-S})_2(\text{CO})_7(\text{PPh}_3)_2]$  (**11**) and **6** in 9%, 29%, 15%, 8% and 5% yields, respectively, in addition to the known compound **4** in 14% yield (Scheme 1).

Table 4

Selected bond distances (Å) and angles (°) for  $[\text{Os}_3(\mu\text{-OH})_2(\text{CO})_8(\text{PPh}_3)_2]$  (**6**)

Os(1)–Os(3)	2.8572(2)
Os(2)–Os(3)	2.8585(2)
Os(1)–Os(2)	3.1197(2)
Os(1)–O(1)	2.140(2)
Os(2)–O(1)	2.126(2)
Os(1)–O(2)	2.148(2)
Os(1)–P(1)	2.3682(8)
Os(2)–P(2)	2.3864(8)
Os(2)–O(2)	2.141(2)
Os(2)–O(2)–Os(1)	93.34(9)
Os(2)–O(1)–Os(1)	93.99(10)
Os(1)–Os(3)–Os(2)	66.160(5)
Os(3)–Os(2)–Os(1)	56.901(4)
C(12)–Os(1)–P(1)	94.05(11)
O(1)–Os(1)–Os(3)	81.64(7)
O(2)–Os(1)–P(1)	93.46(6)
O(1)–Os(2)–P(2)	98.28(7)
O(1)–Os(2)–O(2)	73.25(9)
O(1)–Os(1)–P(1)	92.67(7)
O(1)–Os(1)–O(2)	72.84(9)
C(11)–Os(1)–P(1)	91.95(11)
O(2)–Os(1)–Os(3)	84.92(6)
P(1)–Os(1)–Os(3)	118.53(2)
C(21)–Os(2)–P(2)	94.02(11)
C(22)–Os(2)–P(2)	90.70(11)
O(2)–Os(2)–Os(3)	85.02(6)
O(2)–Os(2)–Os(3)	85.02(6)
O(1)–Os(2)–Os(3)	81.83(7)
O(2)–Os(1)–Os(3)	84.92(6)
O(2)–Os(2)–P(2)	93.49(6)

$[\text{Os}_3(\mu_3\text{-S})(\mu\text{-CO})(\text{CO})_7(\text{PPh}_3)_2]$  (**9**),  $[\text{Os}_3(\mu_3\text{-S})_2(\text{CO})_7(\text{PPh}_3)_2]$  (**11**) and **6** in 9%, 29%, 15%, 8% and 5% yields, respectively, in addition to the known compound **4** in 14% yield (Scheme 1).

The solid-state molecular structure of compound **8** (Fig. 5 and Table 5) consists of a closed  $\text{Os}_3$  triangle with three CO ligands bonded to each Os atom, a  $\mu_3\text{-S}$  ligand and a  $\text{PPh}_3$  ligand. The  $\text{Os}(2)\text{--Os}(3)$  bond [2.7531(3) Å] is the shortest while the  $\text{Os}(1)\text{--Os}(2)$  bond *trans* to  $\text{PPh}_3$  [2.8214(4) Å] is the longest. Two of the three CO ligands attached to  $\text{Os}(1)$  are semi-bridged to an adjacent Os centre with  $\text{Os}(2)\cdots\text{C}(11)$  and  $\text{Os}(3)\cdots\text{C}(13)$  distances of 2.682 and 2.581 Å, respectively, and  $\text{O}(13)\text{--C}(13)\text{--Os}(1)$  and  $\text{O}(11)\text{--C}(11)\text{--Os}(1)$  angles of  $159.8(5)^\circ$  and  $163.7(4)^\circ$ , respectively. The semibridging mode is due to the sterically congested and electron-rich nature of  $\text{Os}(1)$ . The  $\mu_3\text{-sulfido}$  ligand is bonded unsymmetrically [ $\text{Os}(2)\text{--S}(1) = 2.3911(11)$ ,  $\text{Os}(1)\text{--S}(1) = 2.4283(12)$  and  $\text{Os}(3)\text{--S}(1) = 2.4041(12)$  Å] but the average  $\text{Os}\text{--S}$  distance [2.411(2) Å] is comparable to those found for the  $\mu_3\text{-S}$  ligands in  $[\text{Os}_3(\mu_3\text{-S})(\mu_3\text{-CO})(\text{CO})_7(\mu\text{-dppm})]$  [2.393(4) Å] [23],  $[\text{Os}_3(\mu_3\text{-S})(\mu_3\text{-CO})(\text{CO})_9]$  [2.378(3) Å] [24],  $[\text{Os}_4(\mu_3\text{-S})(\text{CO})_{12}]$  [2.381(3) Å] [25] and  $[\text{Os}_3(\mu_3\text{-Se})(\mu_3\text{-CO})(\text{CO})_7(\mu\text{-dppm})]$  [2.5123(14)–2.5302(15) Å] [10]. The  $\text{PPh}_3$  ligand is coordinated to  $\text{Os}(1)$  in an equatorial position. The  $^{31}\text{P}\{^1\text{H}\}$  NMR spectrum contains a singlet at  $\delta$  8.0 and the MS shows the molecular ion at  $m/z$  1118.

By analogy with the formation of  $[\text{Os}_6(\mu_3\text{-Se})_4(\text{CO})_{12}(\mu\text{-dppm})_2]$  [10] by treatment of  $[\text{Os}_3(\mu_3\text{-Se})_2(\text{CO})_7(\mu\text{-dppm})]$  with  $\text{Me}_3\text{NO}$ , and  $[\text{Ru}_6(\mu_3\text{-Se})_4(\text{CO})_{12}(\mu\text{-dppm})_2]$  [5b] by treatment of  $[\text{Ru}_3(\mu_3\text{-Se})_2(\text{CO})_7(\mu\text{-dppm})]$  with  $\text{Me}_3\text{NO}$ , it was considered that the reaction of **2** with

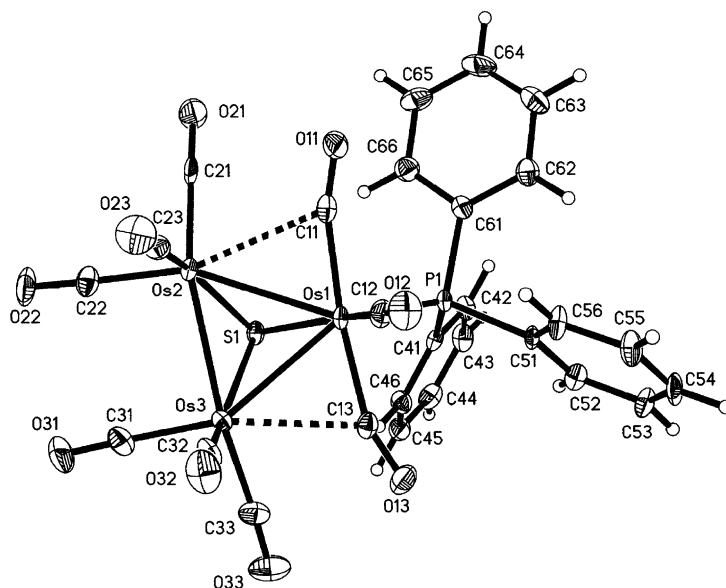


Fig. 5. Solid-state molecular structure of  $[\text{Os}_3(\mu_3\text{-S})(\mu\text{-CO})_2(\text{CO})_7(\text{PPh}_3)]$  (**8**). Thermal ellipsoids are drawn at the 50% probability level.

Table 5

Selected bond distances (Å) and angles (°) for  $[\text{Os}_3(\mu_3\text{-S})(\mu\text{-CO})_2(\text{CO})_7(\text{PPh}_3)]$  (**8**)

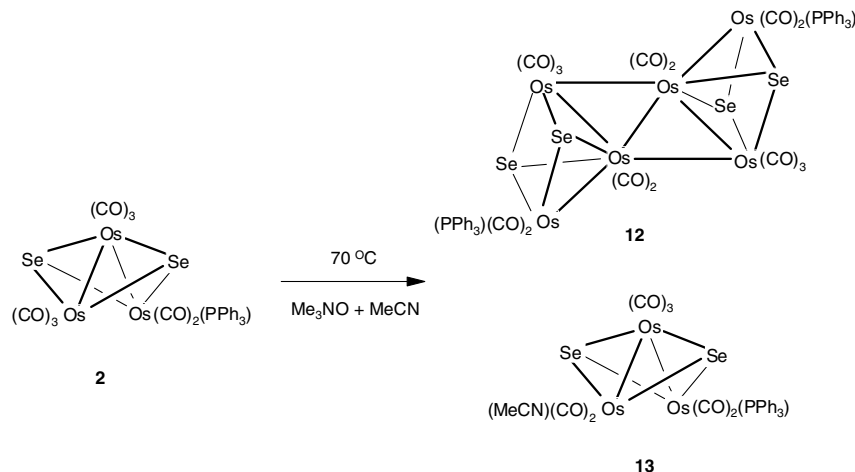
Os(1)–Os(3)	2.7948(3)
Os(2)–Os(3)	2.7531(3)
Os(1)–Os(2)	2.8214(4)
Os(1)–S(1)	2.4283(12)
Os(2)–S(1)	2.3911(11)
Os(3)–S(1)	2.4041(12)
Os(1)–P(1)	2.3727(12)
Os(1)–C(11)	1.958(5)
Os(2)–C(11)	2.682
Os(1)–C(13)	1.968(5)
Os(3)–C(13)	2.5816(5)
Os(3)–Os(1)–Os(2)	58.707(7)
Os(3)–Os(2)–Os(1)	60.164(7)
Os(2)–Os(3)–Os(1)	61.129 (7)
S(1)–Os(1)–Os(3)	54.26(3)
S(1)–Os(2)–Os(3)	55.18(3)
S(1)–Os(2)–Os(1)	54.78(3)
S(1)–Os(1)–Os(2)	53.56(3)
S(1)–Os(3)–Os(1)	55.07(3)
S(1)–Os(3)–Os(2)	54.74(3)
P(1)–Os(1)–Os(3)	133.03(3)
P(1)–Os(1)–Os(2)	136.22(3)
P(1)–Os(1)–S(1)	96.27(4)
Os(2)–S(1)–Os(3)	70.08(3)
Os(3)–S(1)–Os(1)	70.66(3)
Os(2)–S(1)–Os(1)	71.66(3)
O(11)–C(11)–Os(1)	163.7(4)
O(13)–C(13)–Os(1)	159.8(5)

$\text{Me}_3\text{NO}$  might give the corresponding hexanuclear compound  $[\text{Os}_6(\mu_3\text{-Se})_4(\text{CO})_{14}(\text{PPh}_3)_2]$  (**12**). Indeed, treatment of  $[\text{Os}_3(\mu_3\text{-Se})_2(\text{CO})_8(\text{PPh}_3)]$  (**2**) with  $\text{Me}_3\text{NO}$  in toluene at 50 °C gave a dark green hexanuclear cluster  $[\text{Os}_6(\mu_3\text{-Se})_4(\text{CO})_{14}(\text{PPh}_3)_2]$  (**12**) and a trinuclear cluster  $[\text{Os}_3(\mu_3\text{-Se})_2(\text{CO})_7(\text{PPh}_3)(\text{NMe}_3)]$  (**13**) in 46% and 32%

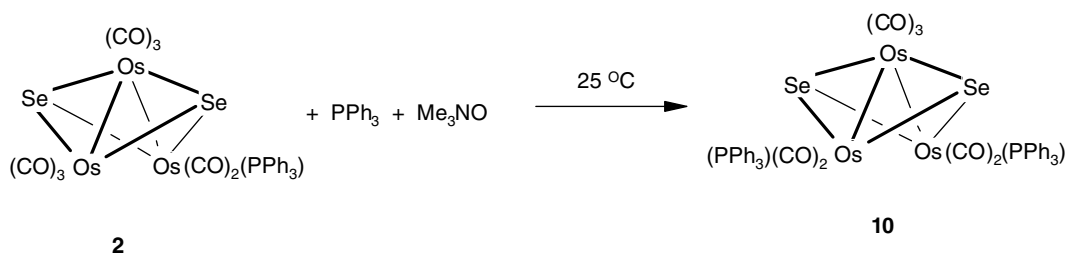
yields, respectively (Scheme 3). Cluster **12** has been characterized by elemental analysis, infrared,  $^1\text{H}$  NMR,  $^{31}\text{P}$  NMR and mass spectra. The singlet at  $\delta$  5.9 in the  $^{31}\text{P}$  NMR spectrum indicates equivalent  $^{31}\text{P}$  nuclei. The FAB MS shows a molecular ion peak at  $m/z$  2374 corresponding to  $[\text{Os}_6(\mu_3\text{-Se})_4(\text{CO})_{14}(\text{PPh}_3)_2]$ . We propose the structure for **12** as shown in Scheme 3.

Compound **13** is formed by oxidation of CO by  $\text{Me}_3\text{NO}$  to give the corresponding  $\text{NMe}_3$  derivative. This reaction is similar to the reported formation of  $[\text{FeCo}_3(\mu\text{-H})(\text{CO})_{11}(\text{NMe}_3)]$  and  $[\text{FeCo}_3(\mu\text{-H})(\text{CO})_{10}(\text{PPh}_2\text{H})(\text{NMe}_3)]$  from the reaction of  $\text{Me}_3\text{NO}$  with  $[\text{FeCo}_3(\mu\text{-H})(\text{CO})_{12}]$  and  $[\text{FeCo}_3(\mu\text{-H})(\text{CO})_{11}(\text{PPh}_2\text{H})]$ , respectively. We grew X-ray quality crystals of **13** but were unable to collect diffraction data because these are unstable. In addition to the usual Ph resonances in the  $^1\text{H}$  NMR spectrum, a singlet at  $\delta$  2.80 is assigned to the  $\text{NMe}_3$  ligand. The  $^{31}\text{P}\{^1\text{H}\}$  NMR spectrum shows a singlet at  $\delta$  13.77. The FAB MS shows a molecular ion peak at  $m/z$  1247 corresponding to  $[\text{Os}_3(\mu_3\text{-Se})_2(\text{CO})_7(\text{PPh}_3)(\text{NMe}_3)]$ .

The reaction of **2** with  $\text{PPh}_3$  and  $\text{Me}_3\text{NO}$  at room temperature results in substitution of one CO ligand to produce  $[\text{Os}_3(\mu_3\text{-Se})_2(\text{CO})_7(\text{PPh}_3)_2]$  (**10**) (Scheme 4) in 44% yield. Compound **10** can also be obtained from the reaction of **1** with  $\text{PPh}_3$  and  $\text{Me}_3\text{NO}$ . Single crystals of **10** for X-ray diffraction were unavailable. The IR spectrum of **10** in  $\text{CH}_2\text{Cl}_2$  is similar to that of  $[\text{Ru}_3(\mu_3\text{-Se})_2(\text{CO})_7(\text{PPh}_3)_2]$ , obtained from the reaction of  $[\text{Ru}_3(\text{CO})_{12}]$  and  $\text{PPh}_3\text{=Se}$  and characterized by X-ray diffraction [7a]. The two phosphorus atoms in **10** are inequivalent, since the  $^{31}\text{P}\{^1\text{H}\}$  NMR spectrum shows singlets at  $\delta$  25.7 and 13.5. The formation of **10** is also confirmed by its FAB mass spectrum ( $m/z$  1450).



Scheme 3.



Scheme 4.

Finally, the treatment of **3** with Se in refluxing toluene gives compound **2** in 38% yield.

In summary, in contrast to the reaction between  $\text{PPh}_3=\text{Se}$  and  $[\text{Ru}_3(\text{CO})_{12}]$ , the reaction of  $[\text{Os}_3(\text{CO})_{10}(\text{MeCN})_2]$  with  $\text{PPh}_3=\text{Se}$  gives six products: three (**2**, **3** and **5**) are monosubstituted phosphine derivatives containing capping Se ligands, two are phosphine-only derivatives (**4** and **6**) and the unsubstituted capped Se compound **1** is also formed. Notably  $[\text{Os}_3(\mu_3\text{-Se})_2(\text{CO})_7(\text{PPh}_3)_2]$ , the osmium analogue of the open triangular  $\text{Ru}_3\text{Se}_2$  *nido* cluster  $[\text{Ru}_3(\mu_3\text{-Se})_2(\text{CO})_7(\text{PPh}_3)_2]$  which was formed in 92% yield, was not detected from the room temperature reaction between  $\text{PPh}_3=\text{Se}$  and  $[\text{Os}_3(\text{CO})_{10}(\text{MeCN})_2]$ . This might be due to the relatively high substitutional lability of the ruthenium carbonyl clusters compared with that of osmium. As shown in Scheme 1 the reaction of  $\text{Ph}_3\text{P}=\text{S}$  with  $[\text{Os}_3(\text{CO})_{10}(\text{MeCN})_2]$  takes a different course in terms of the formation of capping sulfido compounds. The details of the initial reaction are still unresolved but it is likely that Os–S or Os–Se bonds are formed initially to give  $[\text{Os}_3(\text{CO})_{10}(\text{MeCN})(\text{Ph}_3\text{PE})]$  which loses  $\text{MeCN}$  to give  $[\text{Os}_3(\mu\text{-EPPH}_3)(\text{CO})_{10}]$ . Cleavage of the  $\text{P}=\text{E}$  bond would lead to free  $\text{PPh}_3$  and further reaction with  $\text{PPh}_3=\text{E}$  would lead to the disulfido and diselenido products. Note that other authors reported the formation of only **3** and  $[\text{Os}_3(\text{CO})_{11}(\text{PPh}_3)]$  with

$\text{Ph}_3\text{P}=\text{Se}$  [11]. They used identical reaction conditions and we are unable to account for their different observations.

### 3. Experimental

All reactions and manipulations were carried out under an atmosphere of purified dinitrogen by using standard Schlenk techniques. All solvents were distilled from appropriate drying agents. IR spectra were recorded on a Shimadzu FTIR 8101 spectrophotometer. NMR spectra were recorded on a Bruker DPX 400 spectrometer. Chemical shifts for the  $^{31}\text{P}\{^1\text{H}\}$  NMR spectra are relative to 85%  $\text{H}_3\text{PO}_4$ . Elemental analyses were carried out by the Microanalytical Laboratory at University College London. The cluster  $[\text{Os}_3(\text{CO})_{10}(\text{MeCN})_2]$  was prepared according to the published method [26]. Fast atom bombardment mass spectra were obtained on a JEOL SX-102 spectrometer using 3-nitrobenzyl alcohol as matrix and CsI as calibrant.

#### 3.1. Reaction of $[\text{Os}_3(\text{CO})_{10}(\text{MeCN})_2]$ with $\text{Ph}_3\text{P}=\text{Se}$

A dichloromethane solution (50 mL) of  $[\text{Os}_3(\text{CO})_{10}(\text{MeCN})_2]$  (0.225 g, 0.241 mmol) and  $\text{Ph}_3\text{P}=\text{Se}$  (0.165

g, 0.482 mmol) was stirred at room temperature for 48 h. The solvent was removed under reduced pressure and the residue dissolved in  $\text{CH}_2\text{Cl}_2$  and separated by TLC on silica. Elution with hexane/ $\text{CH}_2\text{Cl}_2$  (10:3 by volume) produced six bands. The first and fourth bands gave the known compounds  $[\text{Os}_3(\mu_3\text{-Se})_2(\text{CO})_9]$  (**1**) (0.028 g, 12%) and  $1,2\text{-}[\text{Os}_3(\text{CO})_{10}(\text{PPh}_3)_2]$  (**4**) (0.023 g, 7%). The third band gave the recently reported cluster  $[\text{Os}_3(\mu_3\text{-Se})(\mu\text{-CO})_2(\text{CO})_7(\text{PPh}_3)]$  (**3**) (0.042 g, 15%) [11] as orange crystals from hexane/ $\text{CH}_2\text{Cl}_2$  at  $-4^\circ\text{C}$  (Calc. for  $\text{C}_{27}\text{H}_{15}\text{O}_9\text{Os}_3\text{PSe}$ : C, 27.86; H, 1.30. Found: C, 27.99; H, 1.42%). IR ( $\nu(\text{CO})$ ,  $\text{CH}_2\text{Cl}_2$ ): 2079s, 2039vs, 2019m, 1990s(br) and 1900br (KBr)  $\text{cm}^{-1}$ ;  $^{31}\text{P}\{^1\text{H}\}$  NMR ( $\text{CDCl}_3$ ):  $\delta$  8.1 (s); mass spectrum:  $m/z$  1164. The second band gave  $[\text{Os}_3(\mu_3\text{-Se})_2(\text{CO})_8(\text{PPh}_3)]$  (**2**) (0.033 g, 10%) as yellow crystals after recrystallization from hexane/ $\text{CH}_2\text{Cl}_2$  at  $-4^\circ\text{C}$  (Calc. for  $\text{C}_{26}\text{H}_{15}\text{O}_8\text{Os}_3\text{PSe}_2$ : C, 25.70; H, 1.25. Found: C, 25.95; H, 1.35%). IR ( $\nu(\text{CO})$ ,  $\text{CH}_2\text{Cl}_2$ ): 2079s, 2046vs, 2015s, 2000s, 1956w  $\text{cm}^{-1}$ ;  $^{31}\text{P}\{^1\text{H}\}$  NMR ( $\text{CDCl}_3$ ):  $\delta$  19.1(s); mass spectrum:  $m/z$  1216. The fifth band gave  $[\text{Os}_3(\mu_3\text{-Se})(\text{CO})_7(\mu_3\text{-CO})(\text{PPh}_3)_2] \cdot \text{CH}_2\text{Cl}_2$  (**5**) (0.057 g, 16%) as yellow crystals from hexane/ $\text{CH}_2\text{Cl}_2$  at  $-4^\circ\text{C}$  (Calc. for  $\text{C}_{45}\text{Cl}_2\text{H}_{32}\text{O}_8\text{Os}_3\text{P}_2\text{Se}$ : C, 36.44; H, 2.18. Found: C, 36.65; H, 2.29%). IR ( $\nu(\text{CO})$ ,  $\text{CH}_2\text{Cl}_2$ ): 2064s, 2019s, 2002vs, 1959w, 1942w  $\text{cm}^{-1}$  plus 1610m (KBr)  $\text{cm}^{-1}$ ;  $^1\text{H}$  NMR ( $\text{CDCl}_3$ ):  $\delta$  7.38 (m, 30H), 5.32 (s, 2H,  $\text{CH}_2\text{Cl}_2$ );  $^{31}\text{P}\{^1\text{H}\}$  NMR ( $-50^\circ\text{C}$ ,  $\text{CDCl}_3$ ):  $\delta$  14.6(s), 7.4(s); mass spectrum:  $m/z$  1398. The slowest moving band gave  $[\text{Os}_3(\mu\text{-OH})_2(\text{CO})_8(\text{PPh}_3)_2]$  (**6**) (0.024 g, 7%) as pale yellow crystals after recrystallization from hexane/ $\text{CH}_2\text{Cl}_2$  at  $-4^\circ\text{C}$  (Calc. for  $\text{C}_{44}\text{H}_{32}\text{O}_{10}\text{Os}_3\text{P}_2$ : C, 39.05; H, 2.39. Found: C, 39.14; H, 2.48%). IR ( $\nu(\text{CO})$ ,  $\text{CH}_2\text{Cl}_2$ ): 2062s, 2002vs, 1983s, 1961w, 1923m plus 3505br (KBr)  $\text{cm}^{-1}$ ;  $^1\text{H}$  NMR ( $\text{CDCl}_3$ ):  $\delta$  7.25 (m, 30H),  $-0.18$  (t, 2H,  $J = 3.6$  Hz);  $^{31}\text{P}\{^1\text{H}\}$  NMR ( $\text{CDCl}_3$ ):  $\delta$  11.6 (s); mass spectrum:  $m/z$  1354.

### 3.2. Reaction of $[\text{Os}_3(\text{CO})_{10}(\text{MeCN})_2]$ with $\text{Ph}_3\text{P}=\text{S}$

A similar reaction to that above of  $[\text{Os}_3(\text{CO})_{10}(\text{MeCN})_2]$  (0.225 g, 0.241 mmol) and  $\text{Ph}_3\text{P}=\text{S}$  (0.142 g, 0.483 mmol) in  $\text{CH}_2\text{Cl}_2$  (50 mL) for 48 h at room temperature followed by similar TLC separation produced six bands which gave the following compounds in order of elution:  $[\text{Os}_3(\mu_3\text{-S})_2(\text{CO})_8(\text{PPh}_3)]$  (**7**) (0.024 g, 9%) (Calc. for  $\text{C}_{26}\text{H}_{15}\text{O}_8\text{Os}_3\text{PS}_2$ : C, 27.85; H, 1.35. Found: C, 28.05; H, 1.42%). IR ( $\nu(\text{CO})$ ,  $\text{CH}_2\text{Cl}_2$ ): 2079s, 2045vs, 2015s, 2000s, 1956m  $\text{cm}^{-1}$ ;  $^{31}\text{P}\{^1\text{H}\}$  NMR ( $\text{CDCl}_3$ ):  $\delta$  19.15(s); mass spectrum:  $m/z$  1122.  $[\text{Os}_3(\mu_3\text{-S})(\mu\text{-CO})_2(\text{CO})_7(\text{PPh}_3)]$  (**8**) (0.078 g, 29%) as (Calc. for  $\text{C}_{27}\text{H}_{15}\text{O}_9\text{Os}_3\text{PS}$ : C, 29.03; H, 1.35. Found: C, 30.15; H, 1.52%). IR ( $\nu(\text{CO})$ ,  $\text{CH}_2\text{Cl}_2$ ): 2079s, 2040vs, 2023m, 1990s(br), 1902w, 1886w  $\text{cm}^{-1}$ ;  $^{31}\text{P}\{^1\text{H}\}$  NMR ( $\text{CDCl}_3$ ):  $\delta$  8.02 (s); mass spectrum:  $m/z$  1118.  $[\text{Os}_3(\text{CO})_{10}(\text{PPh}_3)_2]$  (**4**) (14%).  $[\text{Os}_3(\text{CO})_7(\mu_3\text{-CO})(\mu_3\text{-S})(\text{PPh}_3)_2]$  (**9**) (0.049 g, 15%) (Calc. for  $\text{C}_{44}\text{H}_{30}\text{O}_8\text{Os}_3\text{P}_2\text{S}$ : C, 39.10; H, 2.24. Found: C, 39.25; H, 2.34%). IR ( $\nu(\text{CO})$ ,  $\text{CH}_2\text{Cl}_2$ ): 2062s, 2019s, 2001vs, 1958w, 1942w  $\text{cm}^{-1}$ ; IR ( $\nu(\text{CO})$ , KBr): 1610m  $\text{cm}^{-1}$ ;  $^{31}\text{P}\{^1\text{H}\}$  NMR ( $\text{CDCl}_3$ ):  $\delta$  9.25 (s); mass spectrum:  $m/z$  1352.  $[\text{Os}_3(\mu_3\text{-S})_2(\text{CO})_7(\text{PPh}_3)_2]$  (**11**) (0.025 g, 8%). (Calc. for  $\text{C}_{43}\text{H}_{30}\text{O}_7\text{Os}_3\text{P}_2\text{S}_2$ : C, 38.1; H, 2.23. Found: C, 38.26; H, 2.38%). IR ( $\nu(\text{CO})$ ,  $\text{CH}_2\text{Cl}_2$ ): 2046vs, 2014vs, 2004vs, 1965vs, 1934s  $\text{cm}^{-1}$ ;  $^{31}\text{P}\{^1\text{H}\}$  NMR ( $\text{CDCl}_3$ ):  $\delta$  25.62(s), 12.95(s); mass spectrum:  $m/z$  1356.  $[\text{Os}_3(\mu\text{-OH})_2(\text{CO})_8(\text{PPh}_3)_2]$  (**6**) (0.019 g, 5%).

$[\text{Os}_3(\mu_3\text{-S})_2(\text{CO})_7(\text{PPh}_3)_2]$  (**11**) (0.025 g, 8%). (Calc. for  $\text{C}_{43}\text{H}_{30}\text{O}_7\text{Os}_3\text{P}_2\text{S}_2$ : C, 38.1; H, 2.23. Found: C, 38.26; H, 2.38%). IR ( $\nu(\text{CO})$ ,  $\text{CH}_2\text{Cl}_2$ ): 2046vs, 2014vs, 2004vs, 1965vs, 1934s  $\text{cm}^{-1}$ ;  $^{31}\text{P}\{^1\text{H}\}$  NMR ( $\text{CDCl}_3$ ):  $\delta$  25.62(s), 12.95(s); mass spectrum:  $m/z$  1356.  $[\text{Os}_3(\mu\text{-OH})_2(\text{CO})_8(\text{PPh}_3)_2]$  (**6**) (0.019 g, 5%).

### 3.3. Thermolysis of compound **2** in the presence of trimethylamine-*N*-oxide

On heating solution of **2** (0.015 g, 0.012 mmol) and  $\text{Me}_3\text{NO} \cdot 2\text{H}_2\text{O}$  (0.003 g, 0.039 mmol) in toluene (20 mL) at  $50^\circ\text{C}$  for 1 h, the color changed from yellow to green. The solvent was pumped off and the residue chromatographed by TLC on silica. Elution with hexane/ $\text{CH}_2\text{Cl}_2$  (2:1 by volume) gave three bands. The faster moving band ( $R_f = 0.82$ ) gave the unreacted starting material **2** (0.002 g). Second band ( $R_f = 0.61$ ) afforded  $[\text{Os}_6(\mu_3\text{-Se})_4(\text{CO})_{14}(\text{PPh}_3)_2]$  (**12**) (0.007 g, 46%) (Calc. for  $\text{C}_{50}\text{H}_{30}\text{O}_{14}\text{Os}_6\text{P}_2\text{Se}_4$ : C, 25.30; H, 1.27. Found: C, 26.12; H, 1.45%). IR ( $\nu(\text{CO})$ ,  $\text{CH}_2\text{Cl}_2$ ): 2066vs, 2023s, 2008s, 1961m, 1923w, 1907w  $\text{cm}^{-1}$ ;  $^1\text{H}$  NMR ( $\text{CD}_2\text{Cl}_2$ ):  $\delta$  7.64(m),  $^{31}\text{P}\{^1\text{H}\}$  NMR ( $\text{CD}_2\text{Cl}_2$ ):  $\delta$  25.9 (s); mass spectrum:  $m/z$  2374. The slower moving band ( $R_f = 0.46$ ) gave  $[\text{Os}_3(\mu_3\text{-Se})_2(\text{CO})_7(\text{PPh}_3)(\text{NMe}_3)]$  (**13**) (0.005 g, 32%) (Calc. for  $\text{C}_{28}\text{H}_{24}\text{O}_7\text{Os}_3\text{PSe}_2\text{N}$ : C, 26.99; H, 1.94; N, 1.13. Found: C, 27.25; H, 2.15; N, 1.34%). IR ( $\nu(\text{CO})$ ,  $\text{CH}_2\text{Cl}_2$ ): 2044s, 1996vs, 1976sh, 1954m, 1886vw  $\text{cm}^{-1}$ ;  $^1\text{H}$  NMR ( $\text{CD}_2\text{Cl}_2$ ): 7.58(m), 7.45(m), 2.80(s);  $\delta$   $^{31}\text{P}\{^1\text{H}\}$  NMR ( $\text{CD}_2\text{Cl}_2$ ):  $\delta$  13.77 (s); mass spectrum:  $m/z$  1247.

### 3.4. Reaction of cluster **2** with $\text{PPh}_3$

$\text{Me}_3\text{NO} \cdot 2\text{H}_2\text{O}$  (0.003 g, 0.040 mmol) was added to a  $\text{CH}_2\text{Cl}_2$  solution (25 mL) of **2** (0.023 g, 0.019 mmol) and  $\text{PPh}_3$  (0.010 g, 0.038 mmol) and the reaction mixture was stirred at room temperature for 2 h. The solution was filtered through a short silica column (4 cm) to remove the excess of  $\text{Me}_3\text{NO}$ . The solvent was removed at reduced pressure and the residue chromatographed by TLC on silica. Elution with hexane/ $\text{CH}_2\text{Cl}_2$  (3:2 by volume) gave two bands. The first gave unreacted **2** (0.003 g) while the second band gave  $[\text{Os}_3(\mu_3\text{-Se})_2(\text{CO})_7(\text{PPh}_3)_2]$  (**10**) (0.012 g, 44%) as orange crystals after recrystallization from hexane/ $\text{CH}_2\text{Cl}_2$  (Calc. for  $\text{C}_{43}\text{H}_{30}\text{O}_7\text{Os}_3\text{P}_2\text{Se}_2$ : C, 35.64; H, 2.09. Found: C, 35.78; H, 2.24%). IR ( $\nu(\text{CO})$ ,  $\text{CH}_2\text{Cl}_2$ ): 2046vs, 2014s, 2000m, 1965m, 1934s  $\text{cm}^{-1}$ ;  $^{31}\text{P}\{^1\text{H}\}$  NMR ( $\text{CDCl}_3$ ):  $\delta$  25.7 (s), 13.5 (s); mass spectrum:  $m/z$  1450.

### 3.5. Reaction of cluster **1** with $PPh_3$

$Me_3NO \cdot 2H_2O$  (0.005 g, 0.067 mmol) was added to a dichloromethane solution (25 mL) of **1** (0.027 g, 0.028 mmol) and  $PPh_3$  (0.015 g, 0.057 mmol) (0.005 g, 0.067 mmol). The solution was stirred at room temperature for 3 h, filtered through a short silica column and the solvent was removed under reduced pressure. Chromatography of the residue by TLC on silica gel, eluting with hexane/ $CH_2Cl_2$  gave a single band which afforded compound **2** (0.010 g, 30%).

### 3.6. Reaction of **3** with elemental selenium

A mixture of **3** (0.020 g, 0.018 mmol) and black selenium (0.040 g, 0.037 mmol) in toluene (25 mL) was heated to reflux for 2 h. The solvent was removed under reduced pressure and the residue chromatographed by TLC on silica. Elution with hexane/ $CH_2Cl_2$  (10:3 by volume) gave a single band which afforded **2** (0.008 g, 38%).

### 3.7. X-ray crystallography for compounds **2**, **5**, **6** and **8**

Intensity data for **5** were obtained using a Bruker Nonius Kappa CCD diffractometer using  $Mo\ K\alpha$  radiation. Data collection and processing were carried out by using the programs COLLECT [27] and DENZO [28]. Data were corrected for absorption effects using SORTAV [29]. Data for complexes **2**, **6** and **8** were obtained on a Bruker SMART APEX CCD diffractometer using  $Mo\ K\alpha$  radiation. Data reduction and integration were carried out with SAINT+ and absorption corrections using SADABS [30].

The structures were solved by direct methods and refined on  $F^2$  by full-matrix least-squares (SHELXTL PLUS V6.10) [30] using all unique data. For all structures, the non-hydrogen atoms were refined anisotropically and the hydrogen atoms were included in calculated positions (riding model) except for the OH hydrogens in **6** which were located and their positions refined. The three phenyl rings in **2** were disordered over two sets of orientations, each 50% populated.

### Acknowledgements

Parts of this work were carried out by SEK at University College London and at Lund University. He gratefully acknowledges the Royal Society (London) for a fellowship to spend time at UCL. A.S. and H.A. acknowledge the Ministry of Science and Technology, Bangladesh for Scholarships. A.J.D. thanks the Wenner-Gren Foundation for a fellowship to work in Lund University. We thank Jon Cobb (King's College London) for recording the  $^{31}P$  VT NMR spectra of compound **5**.

### Appendix A. Supplementary material

The crystal data, details of data collection and refinement results are summarised in Table 1. Crystallographic data have been deposited with the Cambridge Crystallographic Data Centre, CCDC Nos 273681 for **2**, 241278 for **5**, 273682 for **6**, and 273683 for **8**. Copies of this information may be obtained free of charge from the Director, CCDC, 12 Union Road, Cambridge CB2 1EZ, UK (fax: +44 1223 336033; e-mail: deposit@ccdc.cam.ac.uk or www: <http://www.ccdc.cam.ac.uk>). Supplementary data associated with this article can be found, in the online version, at doi:10.1016/j.jorgchem.2005.07.038.

### References

- [1] (a) M. Hidai, S. Kuwata, Y. Mizobe, *Acc. Chem. Res.* 33 (2000) 46;  
(b) M. Oakzaki, M. Yuki, K. Kuge, H. Ogino, *Coord. Chem. Rev.* 198 (2000) 367;  
(c) L.C. Roof, J.W. Kolis, *Chem. Rev.* 93 (1993) 1037;  
(d) P. Mathur, *Adv. Organomet. Chem.* 41 (1997) 24.
- [2] (a) M.L. Steigerwald, *Polyhedron* 13 (1994) 1245;  
(b) S.W. Audi Fong, T.S.A. Hor, *J. Chem. Soc., Dalton Trans.* (1999) 639;  
(c) T. Shihara, *Coord. Chem. Rev.* 123 (1993) 73;  
(d) K.H. Whitmire, *J. Coord. Chem.* 17 (1998) 95;  
(e) G. Longoni, M.C. Iapalucci, *Clusters and Colloids*, VCH, Weinheim, 1994, p. 132;  
(f) M.L. Steigerwald, T. Siegrist, E.M. Gyorgy, B. Hessen, Y.-U. Kwon, S.M. Tanzler, *Inorg. Chem.* 33 (1994) 3389;  
(g) S. Ulvenlund, A. Bengtsson-Kloo, in: P. Braunstein, L.A. Oro, P.R. Raithby (Eds.), *Metal Clusters in Chemistry*, vol. 1, VCH, Weinheim, 1999, p. 561;  
(h) D. Fenske, J.F. Corrigan, in: P. Braunstein, L.A. Oro, P.R. Raithby (Eds.), *Metal Clusters in Chemistry*, vol. 3, VCH, Weinheim, 1999, p. 1302.
- [3] (a) T. Akter, N. Begum, D.T. Haworth, D.W. Bennett, S.E. Kabir, Md.A. Miah, N.C. Sarker, T.A. Siddiquee, E. Rosenberg, *J. Organomet. Chem.* 689 (2004) 2571;  
(b) R.D. Adams, M. Tasi, *J. Cluster Sci.* 1 (1990) 249;  
(c) R.D. Adams, *Polyhedron* 4 (1985) 2003;  
(d) R.D. Adams, I.T. Horvath, L.W. Yang, *J. Am. Chem. Soc.* 105 (1983) 1533;  
(e) R.D. Adams, I.T. Horvath, P. Mathur, B.E. Segmuller, *Organometallics* 2 (1983) 996;  
(f) R.D. Adams, I.T. Horvath, P. Mathur, B.E. Segmuller, L.W. Yang, *Organometallics* 2 (1983) 1078;  
(g) R.D. Adams, Z. Dawoodi, D.F. Foust, *Organometallics* 1 (1982) 411.
- [4] (a) D.A. Lesch, T.B. Rauchfuss, *Organometallics* 1 (1992) 499;  
(b) J.G. Brennan, T. Siegrist, S.M. Stuczynski, M.L. Steigerwald, *J. Am. Chem. Soc.* 111 (1989) 9240;  
(c) Z. Nomikou, B. Schubert, R. Hoffmann, M.L. Steigerwald, *Inorg. Chem.* 31 (1992) 2201;  
(d) M.L. Steigerwald, T. Siegrist, S.M. Stuczynski, *Inorg. Chem.* 30 (1991) 4940.
- [5] (a) D. Cauzzi, C. Graiff, C. Massera, G. Mori, G. Predieri, A. Tiripicchio, *J. Chem. Soc., Dalton Trans.* 7 (1998) 321;  
(b) D. Cauzzi, C. Graiff, G. Predieri, A. Tiripicchio, C. Vignali, *J. Chem. Soc., Dalton Trans.* (1999) 237.

- [6] J. Lewis, B.F.G. Johnson, P.G. Lodge, P.R. Raithby, *J. Chem. Soc., Chem. Commun.* (1979) 719.
- [7] (a) P. Baistrocchi, D. Cauzzi, M. Lanfranchi, G. Predieri, A. Tiripicchio, M. Tiripicchio Camellini, *Inorg. Chim. Acta* 235 (1995) 173;  
(b) D. Cauzzi, C. Graiff, M. Lanfranchi, G. Predieri, A. Tiripicchio, *J. Chem. Soc., Dalton Trans.* (1995) 2321;  
(c) P. Baistrocchi, M. Careri, D. Cauzzi, C. Graiff, M. Lanfranchi, P. Manini, G. Predieri, A. Tiripicchio, *Inorg. Chim. Acta* 252 (1996) 367;  
(d) D. Cauzzi, C. Graiff, G. Predieri, A. Tiripicchio, *J. Cluster Sci.* 12 (2001) 259;  
(e) D. Cauzzi, C. Graiff, C. Massera, G. Predieri, A. Tiripicchio, *Inorg. Chim. Acta* 300–302 (2000) 471.
- [8] R.D. Adams, O.-S. Kwon, S. Sanyal, *J. Organomet. Chem.* 681 (2003) 258.
- [9] P. Braunstein, C. Graiff, C. Massera, G. Predieri, J. Rose, A. Tiripicchio, *Inorg. Chim. Acta* 41 (2002) 1372.
- [10] S.E. Kabir, S. Pervin, N.C. Sarker, A. Yesmin, A. Sharmin, T.A. Siddiquee, D.T. Haworth, D.W. Bennett, K.M.A. Malik, *J. Organomet. Chem.* 681 (2003) 237.
- [11] W.K. Leong, W.L.J. Leong, J. Zhang, *J. Chem. Soc., Dalton Trans.* 9 (2001) 1087.
- [12] E.N.-M. Ho, W.-T. Wong, *J. Chem. Soc., Dalton Trans.* (1997) 915.
- [13] R.D. Adams, I.T. Horvath, B.E. Segmuller, L.W. Yang, *Organometallics* 2 (1983) 144.
- [14] D.W. Knoepfel, J.-H. Chung, S.G. Shore, *Acta Crystallogr., Sect. C* 51 (1995) 42.
- [15] E.J. Ditzel, M.P. Gomez-Sal, B.F.G. Johnson, J. Lewis, P.R. Raithby, *J. Chem. Soc.* (1987) 1623.
- [16] S.R. Hodge, B.F.G. Johnson, J. Lewis, P.R. Raithby, *J. Chem. Soc., Dalton Trans.* (1987) 931.
- [17] A.J. Deeming, D.M. Speel, M. Stchedroff, *Organometallics* 16 (1997) 6004.
- [18] M. Hasan, Ph. D. Thesis, Jahangirnagar University, 2003.
- [19] K.A. Azam, R. Dilshad, S.E. Kabir, R. Miah, M. Shahiduzzaman, E. Rosenberg, K. Hardcastle, M.B. Hursthouse, K.M.A. Malik, *J. Cluster Sci.* 7 (1996) 49.
- [20] W.G.-Y. Ho, W.-T. Wong, *Polyhedron* 14 (1995) 2849.
- [21] S.-M. Lee, W.-T. Wong, *J. Cluster Sci.* 7 (1996) 37.
- [22] S.M.T. Abedin, K.A. Azam, M.B. Hursthouse, S.E. Kabir, K.M.A. Malik, R. Miah, H. Vahrenkamp, *J. Organomet. Chem.* 564 (1998) 133.
- [23] K.A. Azam, G.M. Golzar Hossain, S.E. Kabir, K.M.A. Malik, Md. A. Mottalib, S. Pervin, N.C. Sarker, *Polyhedron* 21 (2002) 38.
- [24] R.D. Adams, I.T. Horvath, H.-S. Kim, *Organometallics* 3 (1984) 584.
- [25] R.D. Adams, D.F. Foust, P. Foust, P. Mathur, *Organometallics* 2 (1983) 990.
- [26] B.F.G. Johnson, J. Lewis, D.A. Pippard, *J. Chem. Soc., Dalton Trans.* 4 (1981) 407.
- [27] R. Hooft, COLLECT data collection software, Nonius B.V. Delft, The Netherlands, 1998.
- [28] Z. Otwinowski, W. Minor, in: C.W. Carter, R.M. Sweet Jr. (Eds.), *Macromolecular Crystallography*, Academic Press, New York, 1997, p. 307.
- [29] R.H. Blessing, *Acta Crystallogr., Sect. A* 51 (1995) 33.
- [30] SMART and SAINT software for CCD diffractometers, version 6.1, Bruker AXS, Madison, WI, 2000.